*Ab initio* theory of native defects in alloys: application to charged N vacancies in $Al_xGa_{1-x}N$



2002 J. Phys.: Condens. Matter 14 2577

(http://iopscience.iop.org/0953-8984/14/10/309)

INSTITUTE OF PHYSICS PUBLISHING JOURNAL OF PHYSICS: CONDENSED MATTER

J. Phys.: Condens. Matter **14** (2002) 2577–2589 PII: S0953-8984(02)31941-6

# *Ab initio* theory of native defects in alloys: application to charged N vacancies in $Al_xGa_{1-x}N$

**L E Ramos[1,2], J Furthmüller[1], F Bechstedt[1], L M R Scolfaro[2] and J R Leite[2]**

[1] Institut für Festkörpertheorie und Theoretische Optik, Friedrich-Schiller-Universität, 07743 Jena, Germany
[2] Universidade de São Paulo, Instituto de Física, Caixa Postal 66318, 05315-970 SP, Brazil

E-mail: lramos@ifto.physik.uni-jena.de

Received 17 December 2001
Published 18 March 2002
Online at stacks.iop.org/JPhysCM/14/2577

**Abstract**

We present calculations of the electronic and atomic structures of neutral and charged nitrogen vacancies in $Al_xGa_{1-x}N$ alloys using a combination of first-principles methods. The treatment of the alloys is based on the generalized quasichemical approach to disorder and composition effects and a cluster expansion to account for the various configurations. The point defects are modelled by supercells which are multiples of the alloy clusters. The total-energy and electronic-structure calculations are performed within the density functional theory and the local spin density approximation. We study the atomic structure, the energetics and the charge-dependent vacancy states for the different clusters versus cation numbers and for the alloys versus composition $x$.

## 1. Introduction

Semiconductor alloys with varying compositions have attracted considerable interest in recent years due to their applications in microelectronic, optoelectronic and photovoltaic devices. They allow us to tailor the bandgaps, band offsets, strain state and other properties in layered systems. The energetics, the phase separation, the atomic structure and the electronic states of ternary (or pseudobinary) $A_xB_{1-x}C$ or $AB_{1-x}C_x$ alloys of compound semiconductors are now well understood on the basis of cluster expansion approaches [1–3]. They can be combined with the so-called generalized quasichemical approximation (GQCA) [4,5]. In these approximations a mixed crystal is divided into an ensemble of clusters. The clusters of a certain class contribute with a composition-dependent fraction to all possible alloy configurations. According to the Connolly–Williams method [6] the configurational average can be replaced by a weighted summation. An alloy property follows as a linear combination of the corresponding properties of the isolated clusters. The clusters can be represented by special quasirandom structures [7] or supercells [4, 8]. These structures allow the combination of the special alloy

  

treatments, cluster expansion approach, GQCA and Connolly–Williams method, with *ab initio* total-energy and electronic-structure calculations based on density functional theory (DFT) [9] within the local density approximation (LDA) [10].

On the other hand, the electrical and optical properties of semiconductors and, hence, their alloys are to a large extent determined by point defects. They may be impurities or native defects such as vacancies or antisites. A characteristic of many point defects is the strong coupling between the electronic structure, which depends on their charge states, and the ionic configuration around the defect. In order to model the structural and electronic behaviour of point defects, a supercell method can also be applied in the alloy case in combination with calculations in the framework of DFT–LDA [11–14]. These studies allow us to derive thermodynamic, structural and electronic properties from total-energy calculations. The quantities of interest are the formation energy of the defect, the defect concentration and the ionization levels of the defect.

Until now no attempts have been made to treat point defects in semiconductor alloys on the same level of approximations as the defect-free alloys and the properties of defects in pure materials. Usually the discussions of point defects are based on results for the pure binary crystals. The composition dependence is only taken into account using arguments of the virtual crystal approximation (VCA) [15–18]. For this reason it is time to unify the state-of-the-art treatments of the semiconductor alloys and point defects in semiconductors.

To demonstrate this unification we consider the charged anion vacancy $V_{\mathrm{N}}^{q}$ in the ternary alloy $\mathrm{Al}_x\mathrm{Ga}_{1-x}\mathrm{N}$. The alloy $\mathrm{Al}_x\mathrm{Ga}_{1-x}\mathrm{N}$ is relatively well understood and an important material in nitride-based optoelectronic devices [19]. This holds for the atomic geometry and the energetics as well as the electronic structure. The two binary compounds GaN and AlN are not very different concerning the ionicity and strength of the chemical bonds. The lattice misfit only amounts to 2.5 and 4.1% for the hexagonal $a$ and $c$ lattice constants, respectively [20].

The nitrogen vacancy is a point defect to be considered in $\mathrm{Al}_x\mathrm{Ga}_{1-x}\mathrm{N}$ from both the physical and technological point of view. This point defect occurs in the chemically ordered anion sublattice of the alloy and, hence, it will be directly influenced by the occupation of the neighbouring cation sites with Ga or Al atoms [21]. The nitrogen vacancy in GaN has been studied using first-principles calculations by several authors [22–24]. The s-like $\mathrm{a}_1$ vacancy state lies as a resonance below the valence band maximum (VBM). The p-like $\mathrm{t}_2$ states are split into a singlet and a doublet state, which both lie as resonances in the conduction bands. The large $\mathrm{t}_2$–$\mathrm{a}_1$ splitting is a peculiar property of GaN. For the neutral vacancy $V_{\mathrm{N}}^{0}$ the electron in the singlet $\mathrm{t}_2$-derived state is transferred to the lower-lying bottom of the conduction band. For Al molar fractions $x > 0.5$ tight-binding calculations [15] showed both vacancy levels, $\mathrm{a}_1$ and $\mathrm{t}_2$, in the fundamental gap of $\mathrm{Al}_x\mathrm{Ga}_{1-x}\mathrm{N}$. The formation energy of the nitrogen vacancy in both GaN [22–26] and AlN [18, 25, 26] is relatively large, though this defect is more likely in GaN [21].

In this paper we present a combination of the cluster expansion and GQCAs for $\mathrm{A}_x\mathrm{B}_{1-x}\mathrm{C}$ alloys and the supercell treatment of point defects. Charged nitrogen vacancies $V_{\mathrm{N}}^{q}$ generated in $\mathrm{Al}_x\mathrm{Ga}_{1-x}\mathrm{N}$ mixed crystals are considered as examples. We study the structure, the energetics and the electronic levels of the point defects in dependence on composition $x$, the charge state $q$ of the defect and the background doping level. The considerations are restricted to the cubic (zinc-blende) structure in the limit of the ordered binary compounds. It has been reported [27] that the wurtzite and the cubic phases show nearly equivalent formation energies and electronic structures for defects. The studies are based on *ab initio* total-energy calculations. All atoms in the supercells are fully relaxed and the spin polarization is taken into account.

The paper is organized as follows. The computational methods and formulae are presented in section 2. In section 3, a detailed analysis of our results is given and several

vacancy properties and the underlying physics are discussed versus composition of the alloy. Finally, a summary is given in section 4.

## 2. Computational approaches

### *2.1. Total-energy calculations*

Our calculations are based on DFT within LDA. After the determination of the atomic geometries the spin polarization is taken into account within the local spin-density approximation (LSDA) [10]. Besides the valence electrons of Ga, Al and N also the shallow Ga 3d core states are treated explicitly. The interaction of the electrons with the atomic cores is treated by non-norm-conserving *ab initio* Vanderbilt pseudopotentials [28]. The use of the ultrasoft pseudopotentials allows a restriction of the plane-wave expansion of the single-particle eigenfunctions by an energy cutoff of 16.2 Ryd. This value has been carefully tested for GaN bulk crystals and their surfaces [29].

The $\boldsymbol{k}$-space integrals are approximated by sums over special-point meshes of the Monkhorst–Pack type [30] in the irreducible part of the Brillouin zone (BZ). The $4 \times 4 \times 4$ mesh for simple cubic (sc) supercells with eight atoms is also used in the case of the sc 64-atom supercells. Explicitly we use the Vienna *ab initio* simulation package [31, 32]. One finds the cubic lattice constant, $a = 4.46$ (4.34) Å, the energy of the direct (indirect) gap, $E_g = 2.01$ (3.29) eV, and chemical potentials $\mu(\mathrm{IIIN}^{theo}_{bulk}) = -13.95$ ($-16.40$) eV/pair, for GaN (AlN) in DFT–LDA quality. Thereby the chemical potentials are taken as the negative cohesive energy. The same procedure gives for the group III metals in fcc structure $\mu(\mathrm{Ga}^{theo}_{bulk}) = -3.58$ eV/atom and $\mu(\mathrm{Al}^{theo}_{bulk}) = -4.19$ eV/atom, in agreement with results of other authors [33]. Apart from the typical LDA overbinding and small variations due to the actual crystal structure, the calculated values approach the experimental values, $\mu(\mathrm{IIIN}^{exp}_{bulk}) = -8.96$ ($-11.52$) eV/pair for GaN (AlN) [34] and $\mu(\mathrm{III}^{exp}_{bulk}) = -2.78$ ($-3.34$) eV/atom for Ga (Al) [35].

### *2.2. Alloy treatment*

In order to describe the random $Al_xGa_{1-x}N$ alloys we follow the cluster expansion approach [1, 2] and GQCA [4]. Details can be found in [19]. On the cation sublattice we consider $N$ sites which are randomly occupied by $N_{\mathrm{Al}} = xN$ and $N_{\mathrm{Ga}} = (1-x)N$ atoms. The system is composed by $M$ clusters of $2n$ atoms ($N = nM$), each of which is treated independently. For a given alloy configuration the clusters are arranged in $(J+1)$ classes with distinct total energies (per pair of atoms) of the clusters, $\epsilon_j$, with $j = 0, 1, \ldots, J$. In each class there are $M_j$ clusters with the same energy $\epsilon_j$. It holds $M = \sum_j M_j$. The fractions $x_j = M_j/M$ of clusters of energy $\epsilon_j$ fulfill $\sum_{j=0}^{J} x_j = 1$. These numbers are subject to a constraint due to the given averaged composition $x$, i.e. the Al molar fraction, as $\sum_{j=0}^{J} n_j x_j = nx$. This relation is a special case of the representation of the configurationally averaged and, hence, composition-dependent (and in general temperature-dependent) value $P(x) = \sum_{j=0}^{J} x_j P_j$ of a property $P$ of interest for the pseudobinary $Al_xGa_{1-x}N$ alloy with mainly compositional disorder.

In the case of the defect-free alloys, suitable clusters are cubes with eight atoms (four nitrogen and four cation atoms) [19]. In this case $n = 4$ holds. There are five kinds $j = 0, \ldots, 4$ ($J = 4$) of cluster and they can be labelled by the number of Al atoms, $n_j = 0$, 1, 2, 3, 4, or the number of Ga atoms, $(n - n_j) = 4, 3, 2, 1, 0$. The five classes are $Al_0Ga_4N_4$, $Al_1Ga_3N_4$, $Al_2Ga_2N_4$, $Al_3Ga_1N_4$ and $Al_4Ga_0N_4$ with $n_j = j = 0, 1, 2, 3, 4$ and $n = J = 4$. The degeneracy factors are $g_j = \binom{4}{j} = 4!/j!(4-j)!$. The characteristic cluster parameters

**Table 1.** Characteristic parameters of eight-atom $Al_jGa_{4-j}N_4$ clusters for simulation of a zinc-blende $Al_xGa_{1-x}N$ alloy. They are the equilibrium lattice constant $a$ (in Å), energy gap $E_g$ (in eV), the isothermal bulk modulus $B$ (in Mbar), its pressure derivative $B'$ and the cluster energy $\epsilon_j$ (in eV/pair).

| Parameter | $Ga_4N_4$ | $Al_1Ga_3N_4$ | $Al_2Ga_2N_4$ | $Al_3Ga_1N_4$ | $Al_4N_4$ |
|---|---|---|---|---|---|
| $a$ | 4.465 | 4.435 | 4.404 | 4.372 | 4.341 |
| $E_g$ | 2.01 | 2.60 | 3.08 | 3.41 | 3.29 |
| $B$ | 1.99 | 2.02 | 2.03 | 2.04 | 2.06 |
| $B'$ | 4.28 | 4.10 | 4.02 | 4.01 | 3.97 |
| $\epsilon_j$ | −13.953 | −14.562 | −15.172 | −15.783 | −16.395 |

are given in table 1. Except for the energy gap these parameters vary monotonically with the number $n_j$ of Al atoms. The reason is the transition from direct to indirect gap going from GaN to AlN. The direct Γ–Γ gap is dramatically opened from 2.01 (GaN) to 4.46 eV (AlN) (in DFT–LDA). On the other hand, the indirect Γ–X gap is rather independent of cation, varying from 3.24 (GaN) to 3.29 eV (AlN). In the $Al_xGa_{1-x}N$ system, the band gap shows a small upward bowing. The values of the bowing factors are $b_{\Gamma X} = 0.69$ eV for the indirect ΓX transition and $b_{\Gamma\Gamma} = 1.34$ eV for the direct ΓΓ transition. In a regular solid solution one finds the probabilities $x_j^0 = g_j x^{n_j}(1-x)^{4-n_j}$ for the occurrence of a cluster of class $j$. The real cluster fractions $x_j$ depend on the energies $\epsilon_j$ and temperature $T$. We verify that in $Al_xGa_{1-x}N$ the temperature-dependent cluster fractions $x_j$ are not much different from the fractions $x_j^0$ in an ideal solid solution. For that reason we fix the growth temperature at $T = 950$ K in the following.

The advantage of the eight-atom cubes as fundamental clusters is the possibility of an easy connection to the supercell method used for the *ab initio* treatment of defects. In the case of nitrogen vacancies, the combination of eight equal cubes with $Al_jGa_{4-j}N_4$ clusters and the same orientation already gives a sufficiently large 64-atom supercell of an sc arrangement. In order to account for the effect of the vacancy generation on the atomic positions, the complete 64-atom cells are relaxed. In comparison with the results of the eight-atom cells, mainly the nitrogen atoms within the 64-atom cell are slightly displaced. The large 64-atom clusters are still statistically independent. No two clusters share the same alloying atom. There are other advantages. The centre atom is again a N atom, which can be removed to create a vacancy. Without a vacancy five cluster classes $j = 0, 1, 2, 3, 4$ still have to be considered with the fractions $x_j$ discussed above.

### *2.3. Defect description*

In order to model vacancies in the framework of the described pseudopotential-plane-wave method we apply a supercell method. This approach also allows us to simulate different charge states $q = 0$, 1+, 2+, 3+ of the nitrogen vacancy $V_N^q$. In these cases electrons are removed from the supercell to a noninteracting reservoir level, where they do not contribute to the exchange–correlation or Hartree potential. A rigid negative background charge density, smeared out over the entire cell, is introduced in order to keep the supercell neutral.

Without vacancy the 64-atom supercell arrangement keeps the five basic types of cluster $j = 0, 1, 2, 3, 4$, but it arranges them in larger complexes. After vacancy creation, the degeneracy $g_j$ may be lifted, if a Jahn–Teller distortion appears. As a consequence of the different possible orientations of the cubes during the arrangement into supercells, different chemical environments occur. The differences are increased after the relaxation of the atomic

positions around the vacancy. Already for ideal binary zinc-blende crystals a reduction of the local point-group symmetry from $T_d$ to $D_{2d}$, $C_{3v}$ or $C_{2v}$ is possible. The possible chemical inequivalence and the geometrical deformation of the cation sublattice then give rise to an energetical splitting of the cluster classes. Instead of $g_j$ degenerate clusters one has in general to consider $g_j$ different configurations. Consequently, the Connolly–Williams representation of configurationally averaged defect properties $P$ has to be generalized to

$$P(x) = \sum_{j=0}^{J} x_j \frac{1}{g_j} \sum_{i=1}^{g_j} P_{ji}. \tag{1}$$

Thereby $P_{ji}$ denotes a property or quantity that depends on the class $j$ of the clusters, which model the pseudobinary alloy, and the possible configuration $i$ around the point defect, which indicates equal arrangements in the limit of defect-free alloys.

In the thermal equilibrium the concentrations of the vacancy $V_N^q$ are determined by their formation energies. According to the formalism of Zhang and Northrup [11] the formation energy of a vacancy $V_N^q$ in a random $Al_xGa_{1-x}N$ alloy should be given by

$$\Omega_f(V_N^q, x, \mu(N), E_F) = E_{tot}(V_N^q, x) - N\mu(Al_xGa_{1-x}N) + \mu(N) + qE_F, \tag{2}$$

where $E_{tot}(V_N^q, x)$ is the weighted total energy of the possible defect supercells, $E_F$ is the Fermi energy and $\mu(Al_xGa_{1-x}N)$ is the chemical potential of the alloy. This follows from the values $E_{tot}(V_N^q, j, i)$ for the different cluster classes $j$ and configurations $i$ using the averaging procedure (1). The chemical potential $\mu(Al_xGa_{1-x}N)$ of the bulk alloy is defined by the total energy of the $2N$-atom supercell divided by the number of pairs and averaged over the alloy configurations, i.e.

$$\mu(Al_xGa_{1-x}N) = \frac{1}{N} \sum_{j=0}^{J} x_j E_{tot}(j) \tag{3}$$

with the total energy $E_{tot}(j)$ of the $2N$-atom cluster with $8j$ Al atoms, $8(4-j)$ Ga atoms and $N = 32$ N atoms (cf table 1).

### *2.4. Chemical potentials*

The description of the chemical potentials in the binary compounds [11–14] can be generalized for ternary alloys. In thermal equilibrium

$$\mu(Al_xGa_{1-x}N) = x\mu(Al) + (1-x)\mu(Ga) + \mu(N) \tag{4}$$

holds. Thus, only the cation or anion chemical potential can be chosen freely. The contributions of $\mu(Al)$ and $\mu(Ga)$ to the cation chemical potential are fixed by the composition. Under extremely cation-rich or N-rich preparation conditions the chemical potentials of the individual elements approach the corresponding bulk values, $\mu(X) = \mu(X_{bulk})$ (X = Al, Ga, N). The choice of the chemical potentials is not completely free but has to obey certain boundary conditions. A major criterion is that the potential for an element is lower than the chemical potential of the corresponding bulk (or molecule for N) since otherwise this element would form the energetically more stable bulk or molecular structure. We set $\mu(N_{bulk}) = \frac{1}{2}\mu(N_2$ molecule). It is therefore convenient to consider deviations $\Delta\mu(X) = \mu(X) - \mu(X_{bulk})$ from these values with zero as the maximum value. The lower boundary of the allowed range is determined by the heat of formation of the ternary alloy

$$\Delta H_f(Al_xGa_{1-x}N) = x\mu(Al_{bulk}) + (1-x)\mu(Ga_{bulk}) + \mu(N_{bulk}) - \mu(Al_xGa_{1-x}N). \tag{5}$$

Relation (5) is written in such a way that the heat of formation describes an exothermic reaction. The combination with the mass action law (equation (4)) leads to

$$x\Delta\mu(\mathrm{Al}) + (1-x)\Delta\mu(\mathrm{Ga}) + \Delta\mu(\mathrm{N}) = -\Delta H_f(\mathrm{Al}_x\mathrm{Ga}_{1-x}\mathrm{N}). \tag{6}$$

N-rich and cation-rich preparation conditions are defined as $\Delta\mu(\mathrm{N}) = 0$ and $x\Delta\mu(\mathrm{Al}) + (1-x)\Delta\mu(\mathrm{Ga}) = 0$, respectively. The heat of formation of the alloys is estimated from measured quantities by $\Delta H_f(\mathrm{Al}_x\mathrm{Ga}_{1-x}\mathrm{N}) = (1.28 + 2.00x)$ eV [34, 35].

The calculated values $\mu(\mathrm{Ga}^{theo}_{bulk})$ and $\mu(\mathrm{Al}^{theo}_{bulk})$ and the estimated heats of formation $\Delta H_f(\mathrm{Al}_x\mathrm{Ga}_{1-x}\mathrm{N})$ are used to derive the chemical potential of the nitrogen atoms in the vacancy formation energy. Equation (2) and the nitrogen chemical potential are also used for materials consisting of only one cluster material $j$ by replacing $x$ by $j/4$.

The formation energy (equation (2)) of charged vacancies also depends on the chemical potential $E_F$ of the electrons. In the case of the ordered binary crystals GaN and AlN one divides this quantity into $E_F = E_V + \varepsilon_F$ with $E_V$ as the VBM of the corresponding zinc-blende crystal. The reduced Fermi energy $\varepsilon_F$ varies in the interval $0 \leqslant \varepsilon_F \leqslant E_g$. The gap energy is replaced by the true one. Adding quasiparticle (QP) corrections of about 1.1 (GaN) and 1.6 eV (AlN) to the DFT–LDA values, it follows that $E_g = 3.1$ (GaN) or 4.9 eV (AlN) [36]. A proper alignment of the VBM is necessary to obtain the position of the defect levels in the supercell approach. We use the lowest s-like energy level, i.e. the valence band minimum. The variation of the Fermi level is more difficult in an alloyed semiconductor because of the disorder-induced tail in the density of states (DOS) close to the top of the 'valence bands' and the bottom of the 'conduction bands'. The corresponding states may pin the Fermi level for strong p- or n-type doping. For that reason in the alloy case we allow $\varepsilon_F$ only to vary between the band edges of the smallest energy gap.

The valence band discontinuity is not known in a cluster calculation. However, we find a rather perfect linear variation of the absolute position of the VBM in the different cluster materials with $j$. Therefore, we also assume a linear variation of the band discontinuities $\Delta E_V(j) = (j/4)\Delta E_V$, where $\Delta E_V = 0.22$ eV is the value between GaN and AlN [29].

### *2.5. Ionization levels*

The formation energies $\Omega_f(V^q_{\mathrm{N}}, x, \mu(\mathrm{N}), E_F)$ are in close relationship to the ionization levels of the defects. An ionization level $(q + 1/q)$ is defined as the position of the Fermi level $E_F$ in the energy gap, at which the charge state of the vacancy changes from the initial state $q + 1$ into the final state $q$ [37]

$$\varepsilon(q + 1/q) = E_{tot}(V^q_{\mathrm{N}}, x) - E_{tot}(V^{q+1}_{\mathrm{N}}, x) - E_V(x). \tag{7}$$

For instance, for $q = 0$ the excitation energy $\varepsilon(1 + /0)$ gives the energy that is necessary to bring an electron from the VBM to the positively charged vacancy, which becomes neutral. The composition-dependent VBM follows in accordance with the Connolly–Williams averaging procedure [6] in equation (1) $E_V(x) = \sum_{j=0}^{J} x_j[E_V(j) + \Delta E_V(j)]$.

The position of the ionization levels allows a characterization of the defect as a donor, an acceptor or neither. One has (i) a pure donor when the level $(q + 1/q)$ lies in the gap but not $(q/q-1)$, (ii) a pure acceptor if $(q/q-1)$ lies in the gap but not $(q+1/q)$ or (iii) an amphoteric defect, i.e. the centre is both donor and acceptor, if both levels $(q/q-1)$ and $(q+1/q)$ are found in the fundamental gap (here that of GaN). We shall consider the ionization levels $(1 + /0)$, $(2 + /1+)$ and $(3 + /2+)$.

In the case of an amphoteric centre $V^q_{\mathrm{N}}$ the energetical distance of the two levels $(q/q-1)$ and $(q + 1/q)$ characterizes the interaction of the electrons occupying the vacancy states.

This can be represented by an effective Coulomb integral, a so-called Hubbard energy $U$. It holds that

$$\begin{aligned} U &= \varepsilon(q/q-1) - \varepsilon(q+1/q) \\ &= E_{tot}(V_N^{q+1}, x) + E_{tot}(V_N^{q-1}, x) - 2E_{tot}(V_N^q, x). \end{aligned} \tag{8}$$

## 3. Results and discussion

### *3.1. Cluster geometries*

First, we study the relaxation of the atoms around the vacancies in the clusters $Al_{8\,j}Ga_{8(4-j)}N_{32}$ of the five classes $j = 0, 1, 2, 3, 4$. We found stable minima on the Born–Oppenheimer total-energy surface in dependence on the symmetry $T_d$, $C_{3v}$ and $D_{2d}$ of the starting configurations. The local symmetry $C_{2v}$ has not been considered because of the restriction to the charge states $q = 0$, 1+, 2+, 3+ of $V_N^q$. Due to the occupation of cation sites with different atoms the true point group symmetry is further reduced and the cluster classes $j$ split into subclasses $i$. In the case of $T_d$ symmetry all clusters in one class remain energetically equivalent. However, in the $C_{3v}$ case the classes $j = 1, 2, 3$ split into two subclasses with three and $[4!/j!(4-j)!-3]$ elements. For $D_{2d}$ symmetry only the class with an equal number of Ga and Al atoms splits into a subclass with two and another one with four energetically equivalent configurations.

Interestingly, the clusters with the lowest energy only occur for starting configurations of nearly $T_d$ symmetry, at least for chemically identical cations. There is no tendency for pairing of two neighbouring cations ($D_{2d}$) or the strong displacement of one cation against the other three neighbours ($C_{3v}$). The reason is that in all considered charge states in $T_d$ symmetry the degenerate single-particle $t_2$ levels lie above the conduction band minimum and remain unoccupied. There is no need for a symmetry-driven reconstruction, i.e. a Jahn–Teller distortion. In the case of nonequivalent vacancy neighbours, the symmetry reduction occurs automatically and is, of course, also accompanied by different atomic displacements. This gives rise to the symmetry reduction discussed above.

Results of the structural optimizations are given in table 2. The atomic displacements of the inequivalent four nearest-neighbour atoms are represented in a local coordinate system, which contains a breathing mode component $b$ along the corresponding body diagonal, a pairing mode component $p_1$ pointing towards another neighbour and a component $p_2$ orthogonal to the two others [14, 38]. The energies of the defect-containing clusters are given with respect to the defect-free clusters. As a reservoir of the nitrogen atoms, the bulk of clusters $Al_jGa_{4-j}N_4$ is assumed. After vacancy ionization the electron is assumed to move into a reservoir given by the VBM of GaN. In other words, according to the definition in equation (2), we list in table 2 the formation energy

$$\Omega_f(V_N^q, j, i) = E_{tot}(V_N^q, j, i) - E_{tot}(j) + \mu(N)|_{cation\text{-}rich} + q[E_V(j) + \Delta E_V(j)] \tag{9}$$

of a charged nitrogen vacancy under cation-rich preparation and rather p-doping conditions in a material of clusters of class $j$ and subclass $i$. Using an atomic starting geometry with $T_d$ symmetry only one subclass exists as in the defect-free case. Calculating the quantities in equation (9) we only apply theoretical values.

In contrast to the cohesive energies (or chemical potentials in table 1) the formation energies of a charged N vacancy under cation-rich and p-doping conditions do not vary too much with the ratio of Ga and Al atoms in the cluster material. In the neutral case, the formation energies are positive. The value of 2.8 eV for $V_N^0$ in GaN is in between those published by Neugebauer and Van de Walle [22, 23] or Mattila and Nieminen [25, 26] and Bogusławski *et al* [24]. There is a tendency for negative values of the positively charged

**Table 2.** Geometrical changes around a vacancy $V_N^q$ in the five classes of equivalent clusters forming the alloy using a $T_d$ starting geometry. The displacements of the four nearest-neighbour cations are given as percentages of the bond length $\sqrt{3}a/4$ in the cluster class $j$ by $b$, $p_1$ and $p_2$ (see section 3.1). The effective formation energy (9) (cation-rich and p-type preparation conditions) is also given (in eV).

| Vacancy | Class | Local symmetry | Nearest neighbours | $b$ (%) | $p_1$ (%) | $p_2$ (%) | $\Omega_f$ (eV) |
|---|---|---|---|---|---|---|---|
| $V_N^0$ | 0 | $T_d$ | Ga, Ga, Ga, Ga | −2.1 | 0.0 | 0.0 | 2.82 |
| | 1 | $C_{3v}$ | Al | 0.5 | 0.0 | 0.0 | 2.85 |
| | | | Ga, Ga | −3.2 | −0.1 | ±0.1 | |
| | | | Ga | −3.2 | 0.1 | 0.0 | |
| | 2 | $C_{2v}$ | Al, Al | −0.6 | −1.6 | 0.0 | 2.82 |
| | | | Ga, Ga | −3.6 | −2.6 | 0.0 | |
| | 3 | $C_{3v}$ | Ga | −3.2 | 0.0 | 0.0 | 2.87 |
| | | | Al, Al | −0.5 | 0.5 | ±1.0 | |
| | | | Al | −0.5 | −1.1 | 0.0 | |
| | 4 | $T_d$ | Al, Al, Al, Al | 1.9 | 0.0 | 0.0 | 2.85 |
| $V_N^{1+}$ | 0 | $T_d$ | Ga, Ga, Ga, Ga | 0.6 | 0.0 | 0.0 | 0.24 |
| | 1 | $C_{3v}$ | Al | 5.6 | 0.0 | 0.0 | 0.00 |
| | | | Ga, Ga | −0.2 | 0.3 | ±0.6 | |
| | | | Ga | −0.2 | −0.7 | 0.0 | |
| | 2 | $C_{2v}$ | Al, Al | 5.2 | −0.7 | 0.0 | −0.15 |
| | | | Ga, Ga | −1.7 | 0.8 | 0.0 | |
| | 3 | $C_{3v}$ | Ga | −3.2 | 0.0 | 0.0 | −0.41 |
| | | | Al, Al | 4.1 | −0.4 | ±0.7 | |
| | | | Al | 4.1 | 0.8 | 0.0 | |
| | 4 | $T_d$ | Al, Al, Al, Al | 2.8 | 0.0 | 0.0 | −0.54 |
| $V_N^{2+}$ | 0 | $T_d$ | Ga, Ga, Ga, Ga | 7.3 | 0.0 | 0.0 | 0.07 |
| | 1 | $C_{3v}$ | Al | 12.1 | 0.0 | 0.0 | −0.29 |
| | | | Ga, Ga | 6.7 | 0.2 | ±0.3 | |
| | | | Ga | 6.7 | −0.3 | 0.0 | |
| | 2 | $C_{2v}$ | Al, Al | 11.9 | −0.4 | 0.0 | −0.47 |
| | | | Ga, Ga | 6.1 | 0.4 | 0.0 | |
| | 3 | $C_{3v}$ | Ga | 5.5 | 0.0 | 0.0 | −0.91 |
| | | | Al, Al | 11.4 | −0.3 | ±0.4 | |
| | | | Al | 11.4 | 0.5 | 0.0 | |
| | 4 | $T_d$ | Al, Al, Al, Al | 10.8 | 0.0 | 0.0 | −1.14 |
| $V_N^{3+}$ | 0 | $T_d$ | Ga, Ga, Ga, Ga | 18.2 | 0.0 | 0.0 | −0.40 |
| | 1 | $C_{3v}$ | Al | 20.5 | 0.0 | 0.0 | −0.85 |
| | | | Ga, Ga, Ga | 18.4 | 0.0 | 0.0 | |
| | 2 | $C_{2v}$ | Al, Al | 20.7 | 0.1 | 0.0 | −1.08 |
| | | | Ga, Ga | 18.5 | −0.1 | 0.0 | |
| | 3 | $C_{3v}$ | Ga | 18.5 | 0.0 | 0.0 | −1.70 |
| | | | Al, Al, Al | 20.8 | 0.0 | 0.0 | |
| | 4 | $T_d$ | Al, Al, Al, Al | 20.8 | 0.0 | 0.0 | −2.12 |

vacancies for all cluster types, at least under cation-rich and p-type preparation conditions. In the case of the twofold positively charged vacancies, one electron remains at the $a_1$ level, so that a nonvanishing magnetization density occurs. In all other cases the magnetization density is practically zero. This is obvious for empty $a_1$ states ($V_N^{3+}$) and $a_1$ levels filled with paired electrons ($V_N^{1+}$). In the $V_N^0$ case the spin polarization vanishes, since the third electron occupies conduction-band states with arbitrary spin orientation.

The geometrical relaxations around the vacancies are characterized by a breathing mode. There are only extremely small deviations from a pure breathing relaxation due to chemical variations of the nearest-neighbour site occupations. The breathing displacements $b$ depend on the charge state and the number of Ga and Al neighbours of the vacancy. In the neutral case we observe a tendency of small inward (outward) breathing relaxation for Ga (Al) atoms. Earlier findings of an outward breathing relaxation in GaN are perhaps a consequence of the smaller 32-atom supercells used [22, 23]. For clusters with both Ga and Al atoms the nonradial atomic displacements may be responsible for the fact that Al atoms around $V_N^0$ in clusters of class $j = 2$ and 3 change the sign of the breathing mode parameter. The difference in the breathing-mode behaviour of Ga and Al atoms around a vacancy may be traced back to the stronger or weaker overlap of the dangling-bond orbitals as in the case of silicon and carbon vacancies in SiC [14]. In the case of charged vacancies, the outward breathing mode is enforced. We observe a general tendency for an increase of the outward breathing parameter $b$ with increasing number of missing electrons.

### *3.2. Energetics*

The vacancy formation energies in the $Al_xGa_{1-x}N$ alloys plotted in figure 1 versus the Al molar fraction $x$ exhibit almost a linear behaviour with the composition. For each composition $x$ the threefold positively charged vacancy should be the dominant defect under p-type preparation conditions. On the other hand, the neutral and single positively charged vacancy are favoured under n-type preparation conditions. Only in the high-n-doping limit is there a drastic change in the formation properties with composition. At about $x = 0.6$ the single positively charged vacancies become more favourable than the neutral ones. However, in this doping limit the nitrogen vacancies cannot occur in appreciable concentrations. Figure 1 exhibits a different behaviour of alloys grown under cation-rich or N-rich conditions. Under cation-rich growth conditions the N vacancy, more strictly speaking $V_N^{3+}$, should play a dominant role.

### *3.3. Single-particle defect states*

In order to discuss the influence of charging of the defect and composition of the alloy on the electronic structure, we study the one-electron DOS around the fundamental gap of the alloy. The DOS allows an easy alignment with that of the defect-free system since the majority of peaks related to the system without vacancy are conserved. Results for vacancies obtained from starting atomic coordinates with $T_d$ symmetry are plotted in figure 2 for the five compositions $x = 0.0$, 0.3, 0.5, 0.7 and 1.0 and the charge states $q = 0$, 1+, 2+ and 3+, following the averaging procedure of equation (1).

Despite the limitations of the DFT–LDA in the exact determination of the empty states with respect to the occupied states, figure 2 gives some insights into the electronic behaviour of the nitrogen vacancy in AlGaN systems. In the GaN case, the single-particle defect states $a_1$ and $t_2$ lie in the valence bands and the conduction bands, respectively. Whereas the $a_1$ states do not give rise to a pronounced peak in the DOSs, this occurs for $t_2$ states. They produce a strong peak (or even double peak due to the vacancy–vacancy interaction within the supercell description) near the bottom of the conduction bands. The fundamental gap of the defect-free system increases with $x$ and at least a fraction of the $t_2$ states occurs in the fundamental gap already for $Al_{0.5}Ga_{0.5}N$. For larger numbers of Al atoms also the $a_1$ state gives rise to a peak in the fundamental gap close to the VBM. In the pure AlN case, the $t_2$ states already overlap with the bulk states from the X point in the BZ.

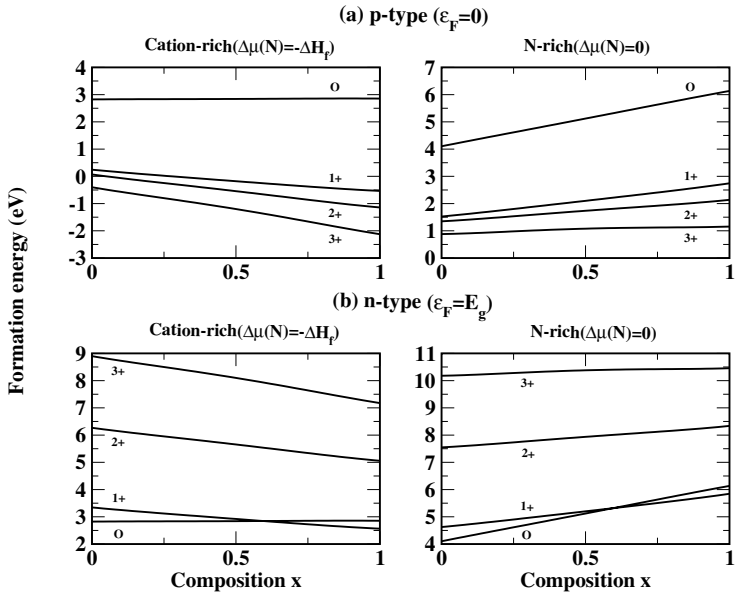


**Figure 1.** Formation energies of charged N vacancies in $Al_xGa_{1-x}N$ versus composition (Al molar fraction $x$) for (*a*) p-type- and (*b*) n-type-preparation conditions.

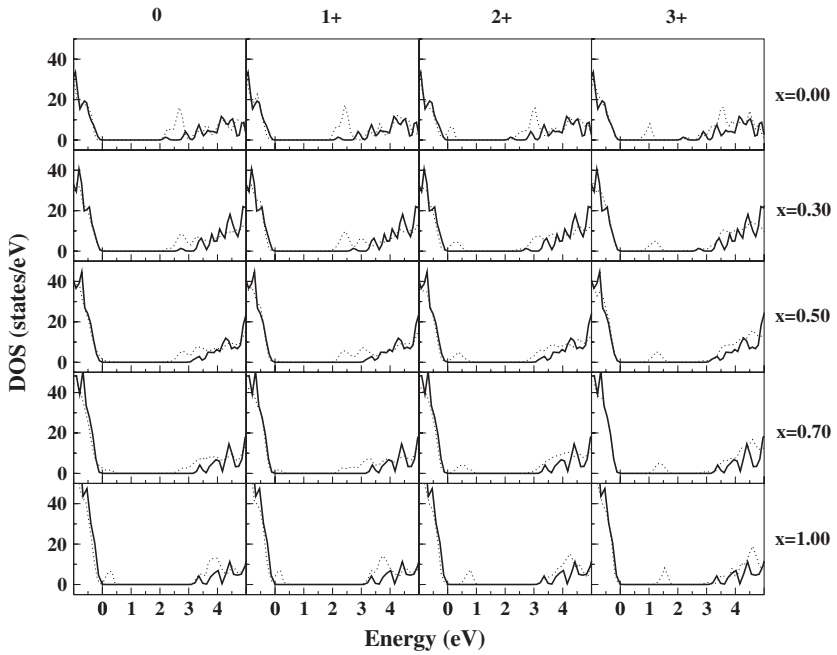


**Figure 2.** Electronic DOS for five compositions $x$ of the $Al_xGa_{1-x}N$ alloy containing a N vacancy (dotted curve) and their respective charged states (0, 1+, 2+ and 3+) in comparison with those of the defect-free materials (solid curve).

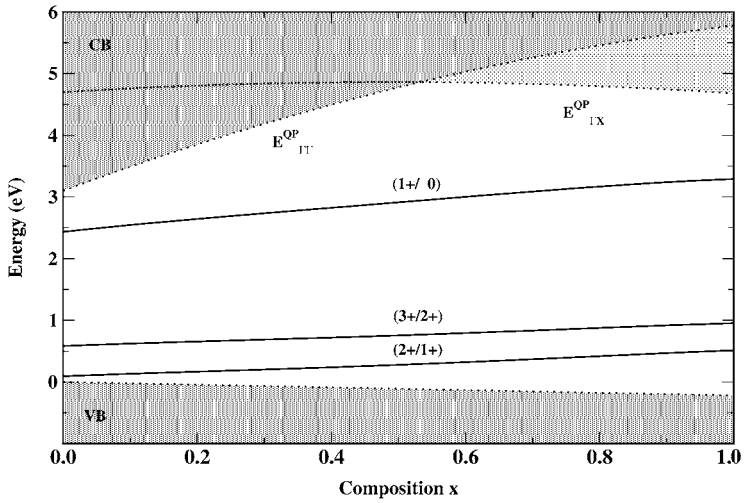


**Figure 3.** Energy-level scheme for the nitrogen vacancy in cubic $Al_xGa_{1-x}N$ alloys versus alloy composition $x$ computed using expression (7). The conduction band edges are plotted taking the QP corrections of [36] into account, whereas the gap bowings are taken from the DFT–LDA calculations.

The DOS in figure 2 exhibits a considerable dependence on the number of electrons occupying the vacancies. There is a general tendency to shift the $a_1$ and $t_2$ states towards higher energies with increasing number of missing vacancy electrons. Only for the change from the $q = 0$ to the 1+ state is this rule broken for the $t_2$ levels. Figure 2 makes obvious that the defect-induced changes happen continuously in the considered chemically disordered $Al_xGa_{1-x}N$ systems. There is a general trend to shift the vacancy states to higher energies not only with the electron loss but also with increasing Al molar fraction in the alloy. This effect is well pronounced for the $a_1$ states, in particular for $q = 2+$ and 3+, where the half-occupied or empty $a_1$ states appear in a midgap position. The tendency is similar in the $t_2$ case. However, in this case, the picture is less clear due to $\boldsymbol{k}$-induced splitting of the $t_2$-bands within the supercell description. The reason is the occupation of conduction band states by one electron in the case of the neutral vacancy. This general shift is specially pronounced for the $a_1$ level. After the loss of all electrons this vacancy state appears in a midgap position in such a way that one may speak about a shallow–deep transition of the defect character.

### *3.4. Ionization levels*

The ionization levels calculated according to expression (7) are plotted versus the Al molar fraction $x$ in figure 3. The three vacancy ionization levels (1 + /0), (2 + /1+) and (3 + /2+) are shown with respect to the band edges, which include a linear interpolation of the QP corrections of GaN and AlN [36]. The VBM is also varied linearly according to the small changes calculated within DFT–LDA for the ionization energies [29]. The conduction-band minima are obtained by adding the QP gaps of the lowest $\Gamma\Gamma$ or $\Gamma X$ transitions [36]. They are linearly interpolated and modified by the bowing factor calculated within the DFT–LDA used here.

Although the (1 + /0) ionization level seems to lie in the gap (figure 3), in reality it occurs much closer to the conduction-band minimum predicted by DFT–LDA without QP corrections (cf the energy gaps shown in table 1). This is a consequence of the occupation, at least partial,

of extended conduction-band states in the neutral case. The ionization levels for the vacancies with fewer electrons are closer to the VBM. These positions represent the strong relationship of the ionization energy $(1+/0)$ to shallow states in the conduction-band minimum and of the ionization energies $(2+/1+)$ and $(3+/2+)$ to the VBM states (cf figures 2 and 3). The defect levels vary monotonically with the composition within the fundamental gap. Their slope is small, in particular for the levels near the VBM. There is an increase of the absolute positions of the levels of about 0.4 eV. This value is small compared with the gap discontinuity of about 1.6 eV but not negligible.

Whereas the single-particle defect levels in figure 2 exhibit a normal behaviour with the charge state of the nitrogen vacancy, the ionization level $(2+/1+)$ lies below the level $(3+/2+)$ in figure 3. It turns out that only the $V_{\mathrm{N}}^{1+}$ and $V_{\mathrm{N}}^{3+}$ charge states of the N vacancy are stable for the entire composition range. Explicitly the ionization levels for GaN are $\varepsilon(1+/0) = 2.43$, $\varepsilon(2+/1+) = 0.09$ and $\varepsilon(3+/2+) = 0.58$ eV, and those for AlN are $\varepsilon(1+/0) = 3.51$, $\varepsilon(2+/1+) = 0.73$ and $\varepsilon(3+/2+) = 1.17$ eV. The effective Coulomb interaction energy $U$ (equation (8)) in the electronic system of the vacancy becomes negative. The variation of $U$ versus composition is weak: for AlN $U = -0.44$ eV and for GaN $U = -0.49$ eV. The average of the two levels $(3+/2+)$ and $(2+/1+)$ gives an ionization level $(3+/1+)$ per electron. The resulting differences to the bottom of conduction bands are 2.7 (GaN) and 4.0 (AlN, indirect) and 5.1 eV (AlN, direct). These values are larger than the centre positions of the broadband luminescence observed at about 2.2–2.3 eV (GaN) or 3.3 eV (AlN) (see [39,40] and references therein).

## 4. Summary

We have developed an *ab initio* treatment of defects in a ternary alloy of the type $\mathrm{A}_x\mathrm{B}_{1-x}\mathrm{C}$, in particular for point defects occupying sites on the chemically ordered anion sublattice. This treatment represents a combination of first-principles methods to describe mixed crystals and defects. The alloy treatment is based on the generalized quasichemical approach to disorder and composition effects and a cluster expansion to account for the various configurations. The point defects are described in supercells which are multiples of the alloy clusters. Alloy and defect studies are performed using total-energy and electronic-structure calculations within a pseudopotential-plane-wave approach. As example defects charged nitrogen vacancies are considered in a cubic $\mathrm{Al}_x\mathrm{Ga}_{1-x}\mathrm{N}$ alloy.

Independent of the charge state and the number of the Al atoms in the various clusters, we do not find a tendency for a remarkable Jahn–Teller distortion. There is only a pronounced breathing mode with mainly outward atomic displacements, which increase with the positive charge of the defect and the number of Al atoms around the vacancy. Distortions of the local $\mathrm{T_d}$ symmetry are due to the inequivalent occupation of the neighbouring cation sites and remain small compared with the breathing-relaxation displacements. We obtained extremely low formation energies for positively charged N vacancies in the p-type limit, in particular, if the alloy is assumed to be grown under cation-rich conditions.

## Acknowledgments

This work was supported by the Deutsche Forschungsgemeinschaft in the framework of the central project 'Group III nitrides and their heterostructures: growth, basic properties and applications' (grant no Be 1346/8-5) and FAPESP, a Brazilian funding agency.

## References


[1] Sanchez J M, Ducastelle F and Gratias D 1984 *Physica* A **128** 334
[2] Zunger A 1994 *Statistics and Dynamics of Alloy Phase Transformations* (New York: Plenum) p 361
[3] Wei S-H, Ferreira L G and Zunger A 1990 *Phys. Rev.* B **41** 8240
[4] Sher A, Van Schilfgaarde M, Chen A-B and Chen W 1987 *Phys. Rev.* B **36** 4279
[5] Chen A-B and Sher A 1995 *Semiconductor Alloys* (New York: Plenum)
[6] Connolly J W D and Williams A R 1983 *Phys. Rev.* B **27** 5169
[7] Zunger A, Wei S-H, Ferreira L G and Bernard J E 1990 *Phys. Rev. Lett.* **65** 353
[8] Bellaiche L, Mattila T, Wang L-W, Wei S-H and Zunger A 1999 *Appl. Phys. Lett.* **74** 1842
[9] Hohenberg P and Kohn W 1964 *Phys. Rev.* B **136** 864
[10] Kohn W and Sham L J 1965 *Phys. Rev.* A **140** 1139
[11] Zhang S B and Northrup J E 1991 *Phys. Rev. Lett.* **67** 2339
[12] García A and Northrup J E 1995 *Phys. Rev. Lett.* **74** 1131
[13] Van de Walle C G, Laks D B, Neumark G F and Pantelides S T 1993 *Phys. Rev.* B **47** 9425
[14] Zywietz A, Furthmüller J and Bechstedt F 1999 *Phys. Rev.* B **59** 15 166
[15] Jenkins D W, Dow J D and Tsai M-H 1992 *J. Appl. Phys.* **72** 4130
[16] Van de Walle C G 1998 *Phys. Rev.* B **57** R2033
[17] McCluskey M D, Johnson N M, Van de Walle C G, Bour D P, Kneissl M and Walukiewicz W 1998 *Phys. Rev. Lett.* **80** 4008
[18] Stampfl C and Van de Walle C G 1998 *Appl. Phys. Lett.* **72** 459
[19] Teles L K, Furthmüller J, Scolfaro L M R, Leite J R and Bechstedt F 2000 *Phys. Rev.* B **62** 2475
[20] Madelung O 1991 *Data in Science and Technology: Semiconductors* (Berlin: Springer)
[21] Bogusławski P and Bernholc J 1999 *Phys. Rev.* B **59** 1567
[22] Neugebauer J and Van de Walle C G 1994 *Phys. Rev.* B **50** 8067
[23] Neugebauer J and Van de Walle C G 1996 *Adv. Solid State Phys.* **35** 25
[24] Bogusławski P, Briggs E L and Bernholc J 1995 *Phys. Rev.* B **51** R17255
[25] Mattila T and Nieminen R M 1996 *Phys. Rev.* B **54** 16 676
[26] Mattila T and Nieminen R M 1997 *Phys. Rev.* B **55** 9571
[27] Neugebauer J and Van de Walle C G 1994 *Proc. Mater. Res. Soc. Symp.* **339** 687
[28] Furthmüller J, Käckell P, Bechstedt F and Kresse G 2000 *Phys. Rev.* B **61** 4576
[29] Grossner U, Furthmüller J and Bechstedt F 1998 *Phys. Rev.* B **58** R1722
[30] Monkhorst H J and Pack J D 1976 *Phys. Rev.* B **13** 5188
[31] Kresse G and Furthmüller J 1996 *Comput. Mater. Sci.* **6** 15
[32] Kresse G and Furthmüller J 1996 *Phys. Rev.* B **54** 11 169
[33] Rapcewicz K, Nardelli M B and Bernholc J 1997 *Phys. Rev.* B **56** R12725
[34] Harrison W A 1989 *Electronic Structure and the Properties of Solids* (New York: Dover)
[35] Kittel C 1966 *Introduction to Solid State Physics* (New York: Wiley)
[36] Rubio A, Corkill J L, Cohen M L, Shirley E L and Louie S G 1993 *Phys. Rev.* B **48** 11 810
[37] Enderlein R and Horing N J M 1997 *Fundamentals of Semiconductor Physics and Devices* (Singapore: World Scientific)
[38] Laasonen K, Nieminen R M and Puska M J 1992 *Phys. Rev.* B **45** 4122
[39] Glaser E R, Kennedy T A, Doverspike K, Rowland L B, Gaskill D K, Freitas J A Jr, Khan M A, Olson D T, Kuznia J N and Wickenden D K 1995 *Phys. Rev.* B **51** 13 326
[40] Youngman R A and Harris J H 1990 *J. Am. Ceram. Soc.* **73** 2338